

Electromagnetic Radiation and in-Medium Effects

Ralf Rapp

Cyclotron Institute and Physics Department, Texas A&M University,
College Station, TX 77843-3366, USA

Received

Abstract. The theory of thermal photon and dilepton emission from a hot and dense hadronic gas, as well as from the Quark-Gluon Plasma, is reviewed in the context of extracting in-medium properties of the matter constituents. In phenomenological applications to ultrarelativistic heavy-ion collisions we focus on recent photon and dilepton spectra as measured by WA98 and CERES/NA45, respectively, at CERN-SPS energies.

Keywords: Quark-Gluon Plasma, Hadrons in Medium, Electromagnetic Probes, Heavy-Ion Collisions

PACS: 25.75.Nq, 25.75.-q, 24.10.Pa

1. Introduction

Among the key objectives in studying the properties of a hot and/or dense strongly interacting medium is the identification of the relevant degrees of freedom that render the most economic description of the pertinent phases of matter. Of special interest are modes that can be connected to (pseudo-) order parameters of the bulk matter. These modes are expected to undergo substantial spectral modifications in the vicinity of phase changes, and thus can be used as indicators of the latter.

Spectacular experimental results have been obtained over the last few years at the Relativistic Heavy-Ion Collider (RHIC) in $Au-Au$ (and $d-Au$) collisions at center-of-mass energies between 63 and 200 AGeV [1, 2, 3, 4]. The emerging consensus is that thermalized bulk matter at energy densities ($\sim 20 \text{ GeV/fm}^3$) well above the critical one ($\sim 1 \text{ GeV/fm}^3$) [5] is being produced in central $Au-Au$ collisions at $\sqrt{s}=200 \text{ AGeV}$, see, *e.g.*, Ref. [6] and references therein. However, the microscopic properties of the produced medium are expected to be thoroughly probed only once electromagnetic (e.m.) and heavy-quark observables become available with high accuracy. In this paper, we constrain ourselves to the former.

The valuable information contained in e.m. spectra from heavy-ion reactions

has clearly been demonstrated at the CERN Super-Proton-Synchrotron (SPS): dilepton and photon spectra from (semi-) central $Pb(158A\text{GeV})\text{-}Pb/Au$ collisions have revealed remarkable excess radiation over baseline sources (such as initial hard $N\text{-}N$ collisions and final-state meson decays) [7, 8, 9]. Theoretical analyses lead to the following conclusions (see, *e.g.*, Refs. [10, 11, 12, 13, 14] for recent reviews): (i) low-mass ($M < 1\text{GeV}$) dilepton spectra require substantial medium modifications of the ρ -meson in hot and dense hadronic matter, with no definite discrimination between a strong broadening as found in hadronic many-body calculations and scenarios based on a dropping ρ -mass; (ii) the predicted prevalence of baryon-driven medium effects has been confirmed experimentally by an increased enhancement at lower SPS energies ($\sqrt{s}=8.7A\text{GeV}$) [15]; (iii) the sensitivity to QGP emission is small at low mass (10-15%); (iv) the same thermal source can account for the excess observed at intermediate dilepton masses ($1\text{GeV} < M < 3\text{ GeV}$) and in direct photon spectra, pointing at initial temperatures of 200-250MeV. Thus, overall, the calculations compared favorably to available data by the year 2002. New data from both WA98 [16] and CERES/NA45 [17] with increased sensitivity to low transverse momenta and high centrality, respectively, are exhibiting excess radiation that could be posing a challenge to theory. An important question to be addressed here is whether these observations are related to an incomplete understanding of the space-time evolution of central $A\text{-}A$ collisions, or if new mechanisms in the microscopic production mechanisms (emission rates) are required.

The remainder of this paper is organized as follows. In Sec. 2 I will give a very brief (and incomplete) survey of theoretical frameworks for evaluating e.m. emission rates (see Ref. [19] for a more detailed recent account), and recall possible connections to chiral symmetry restoration. Sec. 3 contains an analysis of the recent measurements of e.m. spectra at the SPS, and an outlook for RHIC. Conclusions can be found in Sec. 4.

2. E.M. Emission Rates and Vector Mesons in Medium

To leading order in $\alpha_{em} = 1/137$, production rates of photons ($M=0$) and dileptons ($M>0$) from a thermal medium are directly related to the (imaginary part of the) e.m. current correlation function (or photon selfenergy) via

$$q_0 \frac{dR_\gamma}{d^3q} = -\frac{\alpha_{em}}{\pi^2} f^B \text{Im}\Pi_{em}(M=0), \quad \frac{dR_{e^+e^-}}{d^4q} = -\frac{\alpha_{em}^2}{M^2\pi^3} f^B \text{Im}\Pi_{em}(M>0) \quad (1)$$

(f^B : Bose distribution), respectively. In the vacuum, $\text{Im}\Pi_{em}(M=0)=0$, whereas $\text{Im}\Pi_{em}(M>0)$ can be determined by $e^+e^- \rightarrow \text{hadrons}$, being characterized by roughly 2 regimes: for $M > M_{dual} \simeq 1.5\text{GeV}$, the perturbative $q\bar{q}$ continuum reproduces the data within $\sim 20\%$, while for $M < M_{dual}$, $\text{Im}\Pi_{em}$ is saturated by the vector mesons ρ^0 , ω and ϕ . Since $\Gamma_{\rho \rightarrow ee} \simeq 11\Gamma_{\omega \rightarrow ee} \simeq 5.5\Gamma_{\phi \rightarrow ee}$ [20], the isospin-1 (ρ) channel largely dominates the thermal rate. This provides favorable conditions in the quest for chiral symmetry restoration, as discussed below.

In the QCD vacuum, the (approximate) $SU(2)_L \otimes SU(2)_R$ chiral symmetry of the QCD Lagrangian is spontaneously broken by the formation of a (scalar) quark condensate, $\langle \bar{q}q \rangle \simeq (-250 \text{ MeV})^3$. While the condensate is not an observable, the spontaneous breaking of chiral symmetry (SBCS) manifests itself in the excitation spectrum of the vacuum through the (mass-) splitting of “chiral partners”. Most prominent examples in the mesonic sector are the non-degeneracy of the pseudo-/scalar (π -“ σ ”) and axial-/vector (ρ - a_1) channels (in the 2-flavor case, the ω is a chiral singlet). Above the critical temperature for chiral restoration, T_c , the spectral densities within a chiral multiplet become degenerate. Thus, medium modifications of the ρ -meson spectral function are hoped to illuminate mechanisms for chiral restoration. It is clear, however, that this requires to establish connections to the a_1 -channel, as encoded, *e.g.*, in the second Weinberg sum rule [21, 22],

$$f_\pi^2 = - \int \frac{ds}{\pi s} (\text{Im}\Pi_V - \text{Im}\Pi_A) , \quad (2)$$

with axial-/vector correlators $\text{Im}\Pi_{V,A} = (m_{\rho,a_1}^4 / g_{\rho,a_1}^2) \text{Im}D_{\rho,a_1}$ using vector dominance (cf. also Ref. [23]). One should note that other realizations of SBCS are possible; *e.g.*, in Ref. [24], employing Hidden Local Symmetry (HLS) to introduce vector mesons into a chiral Lagrangian, the chiral partner of the pion has been identified with the longitudinal component of the ρ -meson field, the so-called “vector manifestation” of chiral symmetry. The bare parameters of the effective Lagrangian ($m_\rho^{(0)}$, F_π , g_ρ) are constrained by matching the 1-loop expanded axial-/vector correlators to an operator product expansion (OPE, for spacelike momenta) at a typical scale of $\Lambda \simeq 1.1 \text{ GeV}$, with no explicit a_1 and “ σ ” degrees of freedom. The bare couplings and masses are then evolved to the on-shell points rendering a satisfactory phenomenology of free decays.

Intense efforts have been devoted in recent years to evaluate modifications of the vector-meson spectral densities in hot and dense hadronic matter, employing mean-field models, finite-temperature chiral loop expansions, or hadronic many-body theory (see Ref. [10] for a review). The reliability of the calculations resides to a large extent on the ability to constrain effective interaction vertices by both symmetry principles (gauge and chiral) and experimental vacuum decay branchings or scattering data (*e.g.*, $\pi N \rightarrow \rho N$ or γN , γA absorption spectra). Information on vector-meson interactions with excited resonances (*e.g.*, ρ - $\Delta(1232)$) is rather limited. However, they are potentially important once thermal abundances are significant (*e.g.*, at $T=170 \text{ MeV}$, N and Δ densities are approximately equal).

In the vector-manifestation scenario [24], it has been argued that two types of medium effects should be accounted for [25]: (i) the standard thermal loop corrections affect the ρ -mass only to order $\mathcal{O}(T^4)$, consistent with earlier findings; (ii) from matching the thermal correlators to the in-medium OPE (with T -dependent quark condensates), it has been inferred that in addition to (i) a reduction of the bare parameters (masses and couplings) is required. This, in particular, leads to a dropping of the ρ (pole-) mass, consistent with the Brown-Rho scenario [13], and a vanishing of the vector-dominance coupling at T_c .

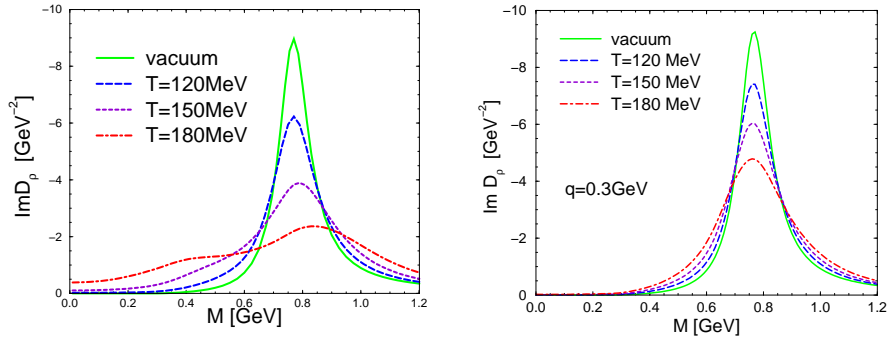


Fig. 1. ρ -meson spectral functions within hadronic many-body theory [26]; left panel: hot+dense matter at temperature [MeV] and baryon density $[\rho_0]$ ($\rho_0=0.16\text{fm}^{-3}$) of $[T, \rho_B] = [0, 0]$ (solid line), $[120, 0.1]$ (long-dashed line), $[150, 0.7]$ (short-dashed line) and $[180, 2.6]$ (dash-dotted line), right panel: hot meson gas.

A typical example of a hadronic many-body calculation of the ρ -meson propagator, $D_\rho = [M^2 - (m_\rho^{(0)})^2 - \Sigma_\rho]^{-1}$, is shown in Fig. 1 (including conservative estimates of contributions from higher resonances) [26]. The essential features, also shared by other calculations of similar kind [27, 28, 29], are: (1) strong broadening of the resonance structure due to large (negative definite) imaginary parts of the in-medium selfenergy, Σ_ρ ; (2) little mass shifts due to cancellations in the real part of Σ_ρ ; (3) prevalence of baryonic over mesonic medium effects (this remains true for net-baryon free matter as long as the total baryon density, $\varrho_{B,tot} = \varrho_B + \varrho_{\bar{B}}$, is significant). The impact of baryons is especially pronounced in the regime below the free ρ -mass, which in thermal dilepton rates is augmented by Bose- and M^{-2} -factors (due to the photon propagator), cf. Eq. (1). Three-momentum integrated dilepton rates from both hadronic gas (HG) and QGP are compiled in the left panel of Fig. 2. One finds that both in-medium rates are strongly enhanced over their free counterparts at low M , a typical many-body effect (and necessary to have a nonzero photon rate for $M \rightarrow 0$). In fact, extrapolating HG and QGP rates (up/down) to $\sim T_c$, rather close agreement emerges, *i.e.*, the “matching” is automatic! Given the importance of baryonic effects, it would be interesting to see whether a more complete treatment of hadronic interactions within the vector manifestation scenario still mandates an “intrinsic” T -dependence of the bare parameters.

Turning to photon production rates (Fig. 2, right panel), the complete leading-order in α_s result has recently been obtained in Ref. [31]; a global enhancement of about a factor 3 over early tree-level estimates [32] has been found. In the hadronic sector, consistency between low-mass dileptons and photon rates has recently been put forward [33]. The processes most relevant for the low-mass enhancement around $M \simeq 0.5\text{GeV}$ dominate the photon rate up to energies of $\sim 1\text{GeV}$. Above, t -channel meson exchanges take over, with formfactor effects reducing the emission strength at high energies appreciably (by a factor ~ 3 at $q_0 \simeq 3\text{GeV}$). In the vicinity of T_c , in-medium QGP and HG rates are again quite comparable in strength.

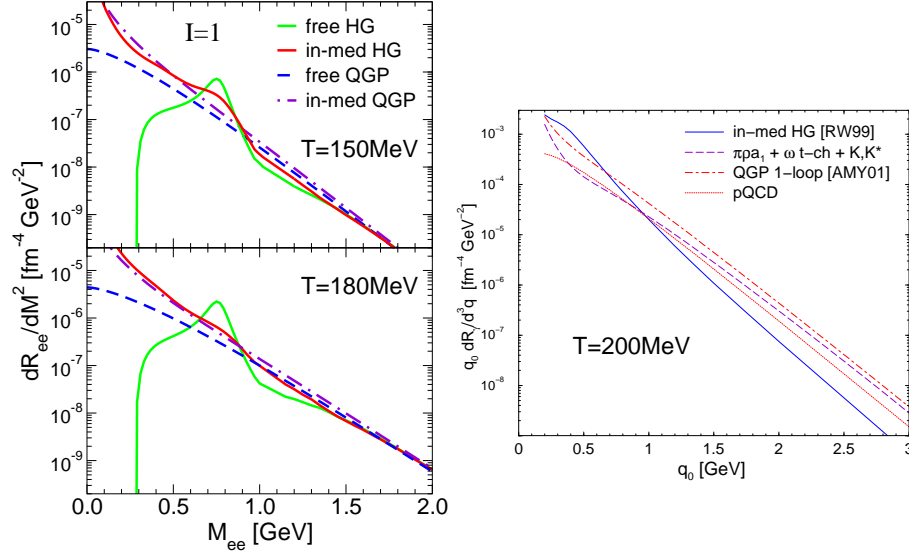


Fig. 2. E.m. emission rates from strongly interacting matter; left panel: dileptons from the isovector channel (dashed and dot-dashed line: free and hard-thermal-loop (HTL) [30] improved $q\bar{q}$ annihilation (QGP), solid lines: free and in-medium hadron gas); right panel: photons (dotted line: tree-level pQCD [32], dash-dotted: complete leading order QGP [31], solid: hadronic many-body contributions at the photon point; dashed: leading order meson-exchange reactions [33]).

3. Electromagnetic Spectra in Heavy-Ion Collisions

To calculate e.m. spectra in heavy-ion collisions, the emission rates are to be convoluted over the space-time history of the reaction, assuming local thermal equilibrium. The selection of results discussed below is based on a simple expanding (isentropic and isotropic) fireball model which is consistent with measured particle yields and radial flow. The resulting photon spectra are, *e.g.*, quite consistent with more elaborate hydrodynamic simulations [34, 35], see also Ref. [14]. The equation of state for the fireball includes finite meson-chemical potentials (μ_π, μ_K , etc.) after chemical freezeout, entailing slightly steeper e.m. spectra (due to faster cooling but with enhanced yields), which is particularly relevant at low M and q_t .

3.1. Photons

The left panel of Fig. 3 shows a comparison of WA98 data from central $Pb-Pb$ at the SPS with a calculation based on the hadronic [33] and complete-LO QGP [31] photon rates displayed in Fig. 2 (right panel). The main points to be made are: (i) prevalence of the primordial contribution from $p-p$ collisions above $q_t \simeq 1.5 \text{ GeV}$ once a moderate Cronin effect (estimated from $p-A$ data) is accounted for, implying

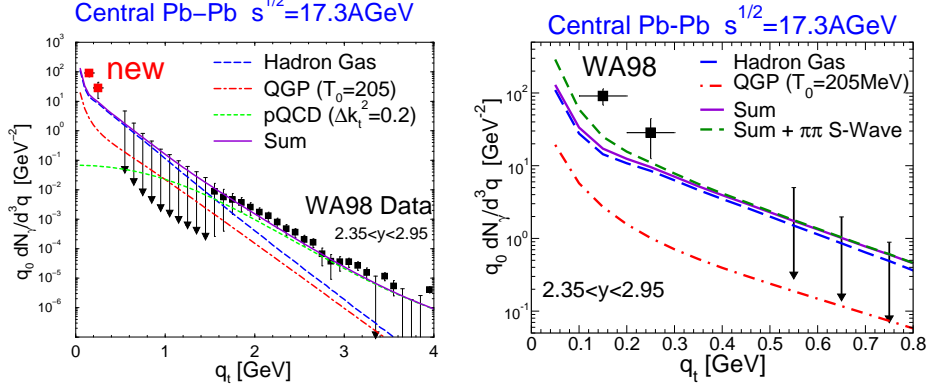


Fig. 3. Direct Photon Spectra as measured in central $Pb(158\text{A GeV})$ - Pb collisions [9, 16] compared to calculations of Ref. [33] (left panel). The right panel magnifies the low-momentum region with the short-dashed line including additional contributions from Bremsstrahlung off free S -wave $\pi\pi$ scattering [36].

that "standard" initial temperatures ($\bar{T}_0 \simeq 205\text{MeV}$ corresponding to a formation time $\tau_0 = 1\text{fm}/c$) for the thermal yield are in line with the data; (ii) consistency with thermal dileptons [10, 19] both in terms of emission rate and space-time evolution; (iii) underestimation of the new low- q_t data by the theory predictions [33, 35]. The latter slightly improve upon inclusion of Bremsstrahlung off S -wave $\pi\pi \rightarrow \pi\pi$ scattering. This opens the exciting possibility that medium effects in the scalar-isoscalar (" σ ") channel are at the origin of the enhancement. However, before conclusions in that direction can be drawn, a thorough evaluation of coherent Bremsstrahlung from the in- and outgoing hadronic charges is mandatory [36].

3.2. Dileptons

In the year 2000, CERES/NA45 measured low-mass e^+e^- with improved statistics and mass resolution over previous results for central $Pb(158\text{A GeV})+Au$ collisions, see left panel of Fig. 4 [17]. The spectra (with the standard single- e^\pm cut $p_t > 0.2\text{GeV}$) are compared to theory predictions for somewhat lower centrality ($N_{ch}=250$), upscaled by the charged-particle multiplicity (i.e., a factor $375/250$; this may slightly overestimate an explicit calculation at $N_{ch}=375$). On the one hand, below the free ρ -mass, conclusions from earlier data are confirmed (cf. Introduction). On the other hand, one now has better sensitivity to the mass regions between the ω and the ϕ , and above the ϕ . For the former, the (broadened) many-body spectral function appears to be favored, although it is not clear whether in the dropping-mass scenario an almost vanishing strength of the e.m. correlator is realistic. Above the ϕ -mass, the original calculations [26] underestimate the data. However, these were based on contributions from 2-pion states only, whereas the free e.m. correlator is known to be dominated by 4-pion (and higher) states above $M_{ee} \simeq 1.2\text{GeV}$ [37]. In addition, vector-axialvector mixing [38, 39] is expected to

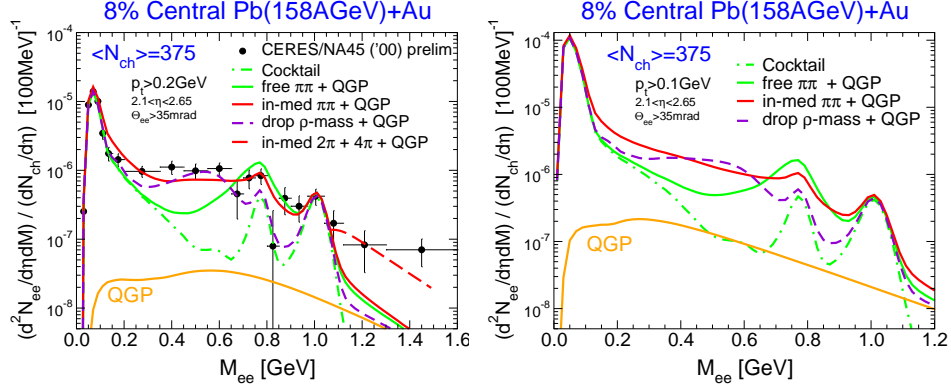


Fig. 4. Left panel: preliminary CERES data (normalized to the π^0 decay) with single- e^\pm cuts $p_t > 0.2 \text{ GeV}$ [17]; theoretical curves [10], added to the final-state decay cocktail (dash-dotted line) [17], are calculated from an expanding fireball with a HG yield using a ρ spectral function with either vacuum shape (green solid line), a dropping mass (short-dashed line), or many-body effects (red solid line), plus a HTL-QGP yield [30]; the long-dashed line for $M > 1.1 \text{ GeV}$ accounts for contributions of $4\text{-}\pi$ states to the e.m. correlator in the hadronic phase. Right panel: theoretical predictions for a reduced single- e^\pm cut of $p_t > 0.1 \text{ GeV}$ (line identification as in the left panel), with the decay cocktail according to Ref. [18].

enhance $\text{Im}\Pi_{em}$ in the mass region between 1 and 1.5 GeV . To schematically include these effects, we have implemented the (“dual”) HTL-improved pQCD rate for the hadronic emission above the ϕ -mass (cf. Fig. 2) with a pertinent 4-pion fugacity factor, $e^{4\mu_\pi/T}$. We have explicitly checked that contributions from Drell-Yan annihilation are small (below the QGP yield), as is also expected for open-charm decays [40]. The approximate agreement with the CERES data above 1 GeV reconfirms the consistency with earlier calculations [41] in the context of the excess observed by NA50 [8].

In view of the low- q_t photon enhancement observed by WA98 and its possible connections to the timelike regime, it is of interest to further probe dileptons at low momentum. In the right panel of Fig. 4 theoretical predictions are given for a reduced single- e^\pm p_t -cut of 0.1 GeV . The most relevant mass range is identified as $M \simeq 0.2\text{--}0.4 \text{ GeV}$, where thermal radiation is still prevalent (below, η and π^0 Dalitz decays take over) and generates a factor $\sim 2\text{--}3$ enhancement over the spectra with $p_t > 0.2 \text{ GeV}$ (at least for the in-medium many-body spectral function). An analysis of the 1996 CERES data with $p_t > 0.1 \text{ GeV}$ for 32% central collisions [42], albeit with rather large statistical errors, is in approximate agreement with these calculations, but more precise data would be very valuable.

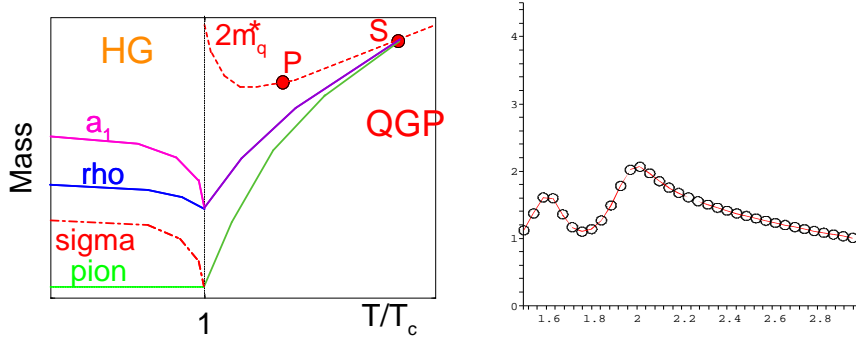


Fig. 5. Left panel: schematic dependence of hadronic masses on temperature [46]. Right panel: ratio of the time-integrated QGP dilepton yield at RHIC from ρ -like bound states [45] to “standard” $q\bar{q}$ annihilation [43]. The two bumps arise from approximately constant-mass ρ -mesons along the “zero-binding line” (higher mass) and from the mixed phase (lower mass). The x -axis denotes invariant dilepton mass in units of the quark quasiparticle mass in the QGP.

3.3. RHIC

Let us finally turn to prospects for RHIC. Due to copious production of open-charm pairs, their correlated semileptonic decay will become a major component in the dilepton spectrum. Nevertheless, due to medium effects on the ρ meson comparable to those at the SPS, the thermal radiation at low mass is expected to outshine the open-charm contribution by a factor ~ 2 -3 [43]. Starting from just above the ϕ -mass, correlated charm decays as extrapolated from p - p spectra [44] dominate over thermal radiation. This situation could change, if (a) charm quarks thermalize in the QGP leading to a softening in the pertinent dilepton M -spectra, and/or (b) the thermal emission rate becomes enhanced. A possible mechanism for the latter has been analyzed in Ref. [45] in terms of “ ρ ”-resonances surviving in the QGP [46] (cf. left panel of Fig. 5), for $T \leq 2T_c$ or so. Depending on their width, an excess of up to a factor 2 over the perturbative QGP emission occurs in the integrated spectra, see right panel of Fig. 5.

4. Conclusions

Electromagnetic probes are providing exciting insights into the properties of hot and dense matter, as produced in relativistic heavy-ion collisions. The theoretical objective is to achieve an accurate enough calculation of the e.m. correlation function that allows a consistent explanation of thermal photon and dilepton spectra. This has to be coupled with a description of the interacting many-body system as a whole, to enable the identification of the relevant degrees of freedom and their chiral properties. In the latter context, the measurement of $\pi^\pm \gamma$ invariant-mass spectra, with the idea to extract spectral properties of the a_1 , would be highly valuable.

Current hadronic calculations exhibit medium effects strong enough to essentially “melt” the light vector mesons (ρ , ω) toward the (pseudo-) phase boundary, rendering a “matching” of the e.m. correlator to structureless pQCD results for the QGP. It will be important to find out in how far nonperturbative interactions in the QGP modify this picture, and at which mass scale they appear.

At the SPS, new dilepton data are so far in reasonable agreement with medium-modified ρ spectral functions, whereas low-momentum photon data indicate an appreciable excess beyond current theoretical expectations. Rather general arguments based on the interplay of temperature and space-time volume relegate the origin of the latter effect to the (late) hadronic phase of central A - A collisions. A softened σ -mode might be a promising candidate to explain these observations. Work in this direction is in progress.

Acknowledgments

I thank U. Mosel for the invitation to a very exciting European Graduate School workshop in Gießen, and J. Wambach for the hospitality during my stay at TU Darmstadt. This work was supported in part by a U.S. National Science Foundation CAREER award under grant PHY-0449489.

References

1. PHENIX Collaboration (K. Adcox *et al.*), e-Print Archive: nucl-ex/0410003.
2. BRAHMS Collaboration (I. Arsene *et al.*), e-Print Archive: nucl-ex/0410020.
3. PHOBOS Collaboration (B.B. Back *et al.*), e-Print Archive: nucl-ex/0410022.
4. STAR Collaboration (J. Adams *et al.*), e-Print Archive: nucl-ex/0501009.
5. F. Karsch and E. Laermann, in R.C Hwa *et al.* (ed.), *Quark gluon plasma*, (2004) 1, and e-Print Archive: hep-lat/0305025.
6. R. Rapp, J. Phys. **G30** (2004) S951.
7. CERES/NA45 Collaboration (G. Agakichiev *et al.*), Phys. Lett. **B422** (1998) 405.
8. NA50 Collaboration (M.C. Abreu *et al.*) Eur. Phys. J. **C14** (2000) 443.
9. WA98 Collaboration (M.M. Aggarwal *et al.*), Phys. Rev. Lett. **85** (2000) 3595.
10. R. Rapp and J. Wambach, *Adv. Nucl. Phys.* **25** (2000) 1.
11. J. Alam *et al.*, Ann. Phys. (NY) **286** (2001) 159.
12. C. Gale and K. Haglin, in R.C. Hwa and X.-N. Wang (eds.), *Quark gluon plasma 3* (2003) 364, and e-Print Archive: hep-ph/0306098.
13. G.E. Brown and M. Rho, Phys. Rep. **398** (2004) 301.
14. R. Rapp, Mod. Phys. Lett. **A19** (2004) 1717.
15. CERES/NA45 Collaboration (D. Adamova *et al.*), Phys. Rev. Lett. **91** (2003) 042301.
16. WA98 Collaboration (M.M. Aggarwal *et al.*), Phys. Rev. Lett. **93** (2004) 022301.

17. CERES/NA45 Collaboration (A. Marin *et al.*), J. Phys. **G30** (2004) S709.
18. H. Appelshäuser *et al.* (CERES/NA45 Collaboration), private communication (2005).
19. R. Rapp, J. Phys. **G** (2005) in press, and e-Print Archive: nucl-th/0409054.
20. Particle Data Group (S. Eidelman *et al.*), Phys. Lett. **B592** (2004) 1.
21. S. Weinberg, Phys. Rev. Lett. **18** (1967) 507.
22. J.I. Kapusta and E.V. Shuryak, Phys. Rev. **D46** (1994) 4694.
23. M. Urban, M. Buballa and J. Wambach, Phys. Rev. Lett. **88** (2002) 042002.
24. M. Harada and K. Yamawaki, Phys. Rep. **381** (2003) 1.
25. M. Harada and C. Sasaki, Phys. Lett. **B537** (2002) 280.
26. R. Rapp and J. Wambach, Eur. Phys. J. **A6** (1999) 415.
27. M. Post, S. Leupold and U. Mosel, Nucl. Phys. **A689** (2001) 753.
28. D. Cabrera, E. Oset and M.J. Vicente-Vacas, Nucl. Phys. **A705** (2002) 90.
29. M.F.M. Lutz, G. Wolf and B. Friman, Nucl. Phys. **A706** (2002) 431.
30. E. Braaten, R.D. Pisarski and T.-C. Yuan, Phys. Rev. Lett. **64** (1990) 2242.
31. P. Arnold, G.D. Moore and L.G. Yaffe, JHEP 0112 (2001) 009.
32. K. Kajantie and H.I. Miettinen, Z. Phys. **C9** (1981) 341.
33. S. Turbide, R. Rapp and C. Gale, Phys. Rev. **C69** (2004) 014903.
34. P. Huovinen, P.V. Ruuskanen and S. Räsänen, Phys. Lett. **B535** (2002) 109.
35. D.K. Srivastava, e-Print Archive: nucl-th/0411041.
36. W. Liu, S. Turbide, R. Rapp and C. Gale, work in progress.
37. ALEPH Collaboration, Eur. Phys. J. **C4** (1998) 409.
38. M. Dey, V.L. Eletsky and B.L. Ioffe, Phys. Lett. **B252** (1990) 620.
39. G. Chanfray, J. Delorme, M. Ericson and M. Rosa-Clot, Phys. Lett. **B455** (1999) 39.
40. P. Braun-Munzinger, D. Miskowiecz, A. Drees and C. Lourenco, Eur. Phys. J. **C1** (1998) 123.
41. R. Rapp and E.V. Shuryak, Phys. Lett. **B473** (2000) 13.
42. G. Hering (CERES/NA45 Collaboration), PhD thesis, Darmstadt University 2001, and e-Print Archive: nucl-ex/0203004.
43. R. Rapp, Proc. of 18th Winter Workshop on Nuclear Dynamics (Nassau, Bahamas, Jan. 20-27, 2002), R. Bellwied, J. Harris and W. Bauer (eds.), EP Systema, Debrecen (Hungary), 283, and e-Print Archive: nucl-th/0204003.
44. R. Averbeck (PHENIX Collaboration), private communication (2001).
45. J. Casalderrey-Solana and E.V. Shuryak, e-Print Archive: hep-ph/0408178.
46. E.V. Shuryak and I. Zahed, Phys. Rev. **C70** (2004) 021901.